Pure & Appl. Chem., Vol. 59, No. 10, pp. 1253–1262, 1987.
Printed in Great Britain.

Enhanced Raman scattering by dielectric spheres

Masahiro Inoue

Institute of Applied Physics, University of Tsukuba, Sakura,
Ibaraki 305, Japan

Abstract - A phenomenon of local field enhancement by dielectric spheres is reviewed. Interaction with surface plasmon polariton of metal substrate is discussed. Especially, a system of a two-dimensional array of spheres placed on a flat substrate is discussed in detail. The obtained features of the resonance modes are shown to be quite general and various possibilities for the application in non-linear optics are suggested.

INTRODUCTION

Electronic and atomic structures of species at crystal surface are studied by scattering or absorption of electromagnetic (EM) field. Vibrational motion of atoms is investigated by absorption of low energy photon or Raman scattering of visible or ultra-violet radiation, while electronic structure is probed by absorption or reflection spectrum. For these purposes, the phenomenon of local field enhancement near the crystal surface is of great convenience, because together with the local field, absorption and scattering efficiencies are also enhanced. Especially, as the enhancement factor being enormous of the order of 10^4–10^6, the surface enhanced Raman scattering (ref. 1) (SERS) by molecules adsorbed on roughened metal surfaces has attracted attention of a vast number of physicists and chemists and various models have been proposed to explain the origin of the enhancement (ref. 2). By now, a consensus seems to be reached that the main origin of this enhancement comes from the enhancement of the local field by the excitation of surface plasmon polariton (SPP) (ref. 3). As the dispersion relation of the SPP lies outside the light cone ($\omega < ck_{||}$, $k_{||}$ being the wavevector component parallel to the surface), it can be excited only when the momentum conservation parallel to the surface is violated by the surface roughness. For both periodic and aperiodic roughened surfaces, model calculations have been performed (ref. 3), which reproduces the qualitative features of the experiments. Observation of surface enhanced absorption, luminescence, second harmonic generation etc. support this model (ref. 3).

Similar enhancement of the local field is attainable even for dielectric materials. When the wavelength of the incident EM field is comparable to the radius of the sphere, a resonance scattering occurs and the local field is enhanced (ref. 4). In this case, retardation effects are essential in contrast to the case of small metal-spheres which is used as a model system to study SERS. The resonance frequency and the enhancement factor depends on the dielectric constant and the radius of the sphere. For materials of usual values of dielectric constants, however, the enhancement factor is not large. Several years ago, we considered a two-dimensional array of dielectric spheres and calculated its optical properties (ref. 5). It was found that the character of the resonance mode of a single sphere is completely changed by the multiple scatterings of EM waves between spheres and the resonance frequency of this system is closely related to that of the localized mode of a thin dielectric slab. The most prominent result (ref. 6) of the calculation is that even for a small dielectric constant, the enhancement factor of the local field intensity turned out to be enormous ($\sim 10^2$), which means that all the optical processes are expected to be enhanced. That is, resonance modes and their associated enhanced local fields can be used to characterize semiconductor and insulator surfaces.

In real systems, spheres are placed on a certain substrate which changes the character of the resonance mode by interaction. The purpose of the present paper is to review the character of the resonance mode itself and the effect of the interaction with the substrate, especially the excitation of the SPP mode on metal surface is discussed in detail. The scope of this paper is as follows. After a brief review of the theory, a single sphere on a metal substrate is considered and the interaction with the SPP mode is discussed. In the next section, a two-dimensional array of dielectric spheres on a flat substrate is discussed in detail. The results are summarized in the last section.

FORMULATION

In this section, we give an outline of the theory and complicated formulas are discarded. Details will be published elsewhere (ref. 7). We assume a local dielectric constant. The Maxwell's equation for the EM field of frequency ω gives a second order differential equation for the electric field,

$$\text{rot rot } E = \nabla\nabla E - \Delta E = \left(\frac{\omega}{c}\right)^2 \varepsilon E, \tag{1}$$

which is equivalent to the integral equation,

$$E(r) = E^0(r) + \int \tilde{G}(r,r')v(r')E(r')\, dr'. \tag{2}$$

The tensor Green's function $\tilde{G}$ and the effective potential for the electric field v are defined by

$$\tilde{G}_{i,j}(r,r') = \left(\delta_{i,j} + \frac{1}{\kappa^2}\nabla_i\nabla_j\right) G(r-r'),$$

$$v(r) = (\kappa^2 - k^2)\theta(r). \tag{3}$$

$$\kappa = \frac{\omega}{c}\sqrt{\varepsilon_0}, \quad k = \frac{\omega}{c}\sqrt{\varepsilon}.$$

G is the usual scalar Green's function. Here, κ and k are the wavevectors in vacuum and in a material of dielectric constant ε, respectively, and the potential vanishes outside the material. This expression shows that, for a material with a larger dielectric constant, the effective potential is more attractive. This ε-dependence is important and determines characteristic features of the resonance mode. To solve this integral equation, the most important step is to find a convenient expression for the tensor Green's function.

In a system with spherical symmetry, EM scattering is described by the vector spherical waves, M and N field (ref. 8).

$$M_{E(f,\kappa,r,L)} = \begin{bmatrix} 0 \\ \frac{1}{\sin\theta}\frac{\partial}{\partial\phi} \\ -\frac{\partial}{\partial\theta} \end{bmatrix} f_\ell(\kappa r)\, Y_L(\hat{r}), \tag{4}$$

$$N_{E(f,\kappa,r,L)} = \begin{bmatrix} \ell(\ell+1)\, f_\ell(\kappa r) \\ (\kappa r\, f_\ell(\kappa r))' \frac{\partial}{\partial\theta} \\ (\kappa r\, f_\ell(\kappa r))' \frac{1}{\sin\theta}\frac{\partial}{\partial\phi} \end{bmatrix} \frac{1}{\kappa r} Y_L(\hat{r})$$

Here the function f_ℓ is a spherical Bessel or a spherical Hankel function of the first kind, and Y_L is the usual spherical harmonic. The capital L (=ℓ,m) denotes both the angular momentum and the magnetic quantum number. With these basis functions, the tensor Green's function is given by (ref. 9)

$$\tilde{G}_{\alpha,\alpha'}(r-r') = \frac{1}{\kappa^2}\delta(r-r')\delta_{\alpha,r}\delta_{\alpha',r}$$

$$- i\kappa\, \beta_{E_\alpha}(f,\kappa,r,L)\, \frac{1}{\ell(\ell+1)}\, \beta^+_{E_{\alpha'}}(g,\kappa,r',L), \tag{5}$$

where $f_\ell(\kappa r) = j_\ell(\kappa r)$, $g_\ell(\kappa r') = h_\ell(\kappa r')$ for $r < r'$,

and $f_\ell(\kappa r) = h_\ell(\kappa r)$, $g_\ell(\kappa r') = j_\ell(\kappa r')$ for $r > r'$,

which is a summation over the angular momentum L for both M and N field. Expanding the incident field by the vector spherical waves, with coefficient $\alpha(0)$, the scattered wave is written by the spherical Hankel function.

$$E^0(r) = {}^{\beta}E(j,\kappa,r,L)\alpha_L^{\beta}(0),$$

$$E^s(r) = {}^{\beta}E(h,\kappa,r,L)\alpha_L^{\beta}(s). \tag{6}$$

Its coefficient $\alpha(s)$ is related to the scattering phase shift of the sphere by

$$\alpha_L^{\beta}(s) = t_{\ell}^{\beta}\alpha_L^{\beta}(0),$$

$$t_{\ell}^{\beta} = \frac{1}{2}\,(\exp(2i\delta_{\ell}^{\beta}) - 1). \tag{7}$$

An important point is for small r, the spherical Hankel function increases by the inverse power of r as $h_{\ell}(\kappa r) \propto 1/(\kappa r)^{\ell+1}$. This is the origin of the local field enhancement. As the enhancement is confined to a rather narrow region near the sphere, it can be interpreted as the counterpart of the evanescent wave excited near a flat metal surface.

On the other hand, for a homogeneous system or a system with a flat surface, vector plane waves are convenient. In this case, the tensor Green's function is written as an integral over the wavevector components parallel to the surface.

$$\tilde{G}_{i,j}(r-r') = \frac{-1}{(2\pi)^3}\int \frac{1}{q^2-\kappa^2}\,(\delta_{i,j} - \frac{1}{\kappa^2}\,q_i q_j)e^{iq(r-r')}dq$$

$$= \frac{1}{\kappa^2}\,\delta(r-r')\delta_{i,z}\delta_{j,z} \tag{8}$$

$$- \frac{i\pi}{(2\pi)^3}\int \frac{1}{\gamma}\,(\delta_{i,j} - \frac{1}{\kappa^2}\,q_i^{\pm}\,q_j^{\pm})e^{iq^{\pm}(r-r')}\,dq_{||}$$

where $\quad q\pm = (q_{||},\ \pm\gamma) \quad z \gtrless z'.$

When the magnitude of $|q_{||}|$ is larger than κ, the z-component γ becomes pure imaginary, and the Green's function represents a propagation of evanescent waves in z-direction. For an incident vector plane wave, either propagating or evanescent, the reflected wave is given by the reflectivity tensor R,

$$E^0(r) = E^0\exp(iq^{-}r),\ E_i^r(r) = R_{i,j}(q)E_j^0\exp(iq^{+}r),$$

$$R_{i,j}(q) = [\frac{\gamma-\gamma'}{\gamma+\gamma'}\,\delta_{i,j} - \frac{2\gamma}{\kappa^2+\gamma\gamma'-\gamma^2}\,\frac{\gamma-\gamma'}{\gamma+\gamma'}\,q_i^{+}\delta_{j,z}$$

$$+ \frac{2\gamma(\gamma-\gamma')^2}{(\gamma+\gamma')(\kappa^2+\gamma\gamma'-\gamma^2)}\,\delta_{i,z}\,\delta_{j,z}]\,e^{2i\gamma Z_0}, \tag{9}$$

where $\quad \gamma = \sqrt{\kappa^2 - q_{||}^2}, \qquad \gamma' = \sqrt{k_2^2-k_{||}^2} \quad = \sqrt{\frac{\omega}{c}^2\varepsilon_2 - k_{||}^2},$

and $\quad q_{||} = k_{||}.$

ε_2 is the dielectric constant of the substrate and γ and γ' are the z-component of the wave vector outside and inside the substrate, respectively.

The difficulty of our system comes from the fact that we need two kinds of basis functions, that is, vector spherical waves for the scattering by a sphere and vector plane waves for the scattering by a substrate. To describe multiple scatterings between a sphere and a substrate, we must rewrite the vector spherical waves from the sphere by a linear combination of the vector plane waves. It is possible if we introduce a new vector ξ, which is a function of wavevector q and angular momentum L.

$$\xi_L^M(q) = A_\ell \begin{bmatrix} 0 \\ \frac{-m}{\sin\theta} Y_L(q) \\ -i \frac{\partial}{\partial\theta} Y_L(q) \end{bmatrix} \qquad \xi_L^N(q) = A_\ell \begin{bmatrix} 0 \\ -\frac{\partial}{\partial\theta} Y_L(q) \\ -i \frac{m}{\sin\theta} Y_L(q) \end{bmatrix} \tag{10}$$

where $A_\ell = \dfrac{4\pi i^{-\ell-1}}{\ell(\ell+1)}$.

Then the tensor Green's function for $z \gtrless z'$

$$\begin{aligned} \tilde{G}_{i,j}(r-r') &= -\frac{i\pi}{(2\pi)^3} \int \frac{1}{\gamma}(\delta_{i,j} + \frac{1}{\kappa^2}\nabla_i\nabla_j) e^{iq^{\pm}(r-r')}\, dq_{||} \\ &= -\frac{i\pi}{(2\pi)^3} \int \frac{1}{\gamma} e^{iq^{\pm}r}\, \xi_L^{\beta}(q^{\pm})\, \beta_E{}^{+}(j,\kappa,r',L)\, dq_{||} \\ &= -\frac{i\pi}{(2\pi)^3} \int \frac{1}{\gamma}\, \beta_E(j,\kappa,r,L)\, \xi_L^{\beta+}(q^{\pm}) e^{-iq^{\pm}r'}\, dq_{||} \end{aligned} \tag{11}$$

represents a conversion of the vector spherical wave into a sum of vector plane waves of both propagating and evanescent and vice versa.

Thus, we have three expressions for the Green's function, which describes a propagation of vector spherical waves, vector plane waves and their mutual conversion. By the use of these expressions, the integral equation is solved exactly and various electromagnetic quantities are calculated.

A DIELECTRIC SPHERE ON A SUBSTRATE

Figure 1 shows the first model we consider, a dielectric sphere of radius a placed on a metal substrate. The distance Z_0 is measured from the center of the sphere to the surface. ε_1 is the dielectric constant of the sphere and ε_2 is that of the substrate.

In Fig. 2, we treat a dielectric sphere in vacuum and substrate is not present here. Abscissa is the scaled frequency ($Z = a/\lambda = \omega a\sqrt{\varepsilon_0}/2\pi c$), which is defined by the radius of the sphere divided by the wave length in vacuum. We show the scattering phase shifts for M and N fields, electric field intensity averaged inside the sphere by a solid curve, normal component of the intensity averaged at slightly outside the sphere by a dotted curve, and the enhancement factor of the Raman intensity by the molecules adsorbed uniformly on the surface by the dashed curve. The Raman tensor is assumed to be diagonal and nonzero only in the direction normal to the surface. The integrated density of states (IDS) (ref. 10) for the EM field is related to the scattering phase shifts by

$$\mathrm{IDS} = \sum_{\ell} (2\ell + 1)\delta_\ell{}^{\beta}/\pi. \tag{12}$$

Then a sharp increase in the phase shifts indicates the presence of a sharp level at that frequency. We call it a resonance mode. When the resonance mode is excited, the local field intensity is enhanced. Increasing the dielectric constant, the effective potential becomes more attractive and the resonance mode shifts to the low frequency side. The spectrum becomes sharp and the enhancement factor increases.

Next, silver is chosen as the substrate and we show in Figs. 3a and 3b the EM energy absorbed inside the metal substrate, which comes from the excitation of the SPP mode. This statement is checked by putting the imaginary part of the dielectric constant of silver to zero. Then the substrate shows total reflection at these frequencies ($\varepsilon_2 < -1$) and the EM energy is transferred only to the SPP mode which propagate to infinity along the substrate surface. For this case, the absorption spectrum changed only a little, which justifies the

statement. The radius and the dielectric constant of the sphere are a = 0.2 μm and ε_1 = 3, respectively. The incidence angle is θ = 45 deg. and the incident field is s-polarized in Fig. 3a and p-polarized in Fig. 3b. The dispersion relation of the SPP mode lies outside the light cone as shown in the inset, so it cannot be exited by the incident field. Therefore, the evanescent wave from the dielectric sphere is the only candidate which can excite the SPP mode. At a large distance (large Z_0), only evanescent waves with small damping constant can reach the substrate. From the energy-momentum conservation, only the SPP modes with small wavevectors or low frequencies can be excited as verified by the dotted curve for Z_0=1 μm. When the sphere approaches the substrate, evanescent waves with larger damping constants can reach the surface and they excite the SPP modes of high

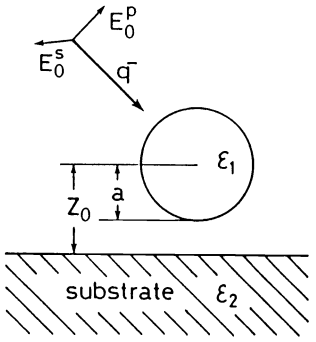

Fig. 1. Geometry of the first model. A dielectric sphere of radius a and dielectric constant ε_1 is placed on a metal substrate of dielectric constant ε_2. The distance Z_0 is measured from the center of the sphere to the surface.

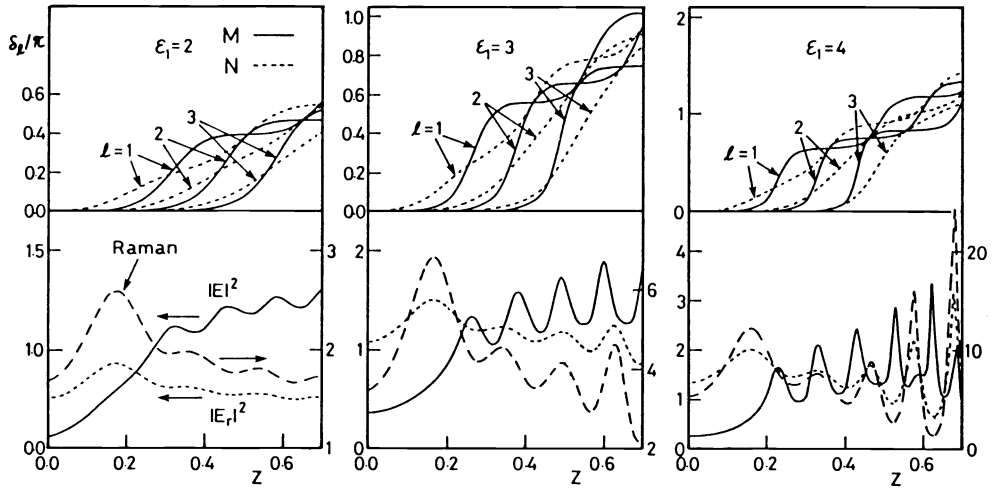

Fig. 2. Scattering phase shifts, electric field intensity averaged inside the sphere, its normal component averaged on the surface, and the enhancement factor of the Raman intensity by the adsorbed molecules for a dielectric sphere in vacuum.

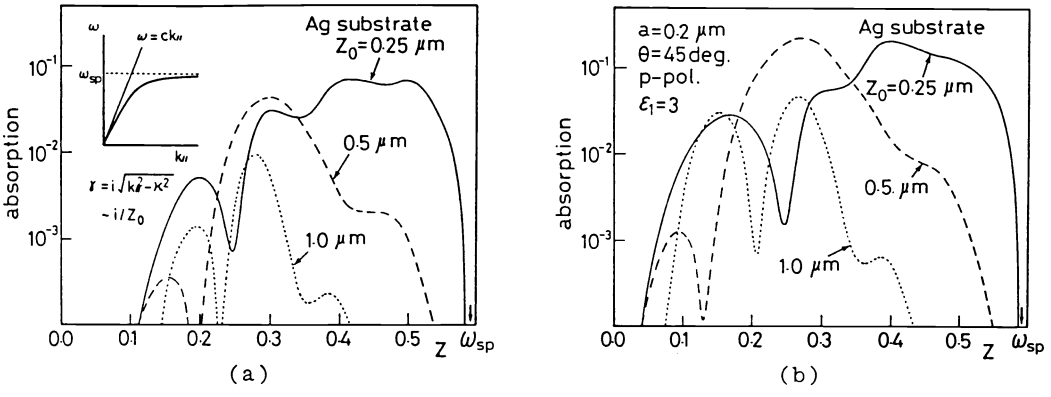

Fig. 3. Distance dependence of the electromagnetic energy absorbed in the metal substrate. (a): s-polarization. (b): p-polarization.

frequencies. As the density of states of the SPP mode increases with the frequency, absorption increases toward the surface plasmon frequency ω_{sp}. Periodic modulation in the spectrum comes from the interference of the incident and the reflected waves. For p-polarization, the absorption increases, especially in the low frequency side. When the wave length is much longer than the radius, the sphere can be replaced by a point dipole and this phenomenon is explained by the dipole radiation model. The emitted dipole field is shown schematically in Fig. 4. In the lower half, the electric vector and the envelope function of the SPP mode are shown. At zero wavevector or at zero frequency, the angle of the electric vector relative to the surface-normal is zero and it increases monotonically to $\pi/4$ at the surface plasmon frequency. Comparing these two figures we can explain the polarization dependence of the absorption spectrum. For s-polarization, the induced dipole is parallel to the surface. Then the electric vector of the dipole radiation is also parallel to the surface, and it is nearly orthogonal to the electric vector of the SPP mode at low frequencies. Because of the orthogonality of the wave functions, the s-polarized incident field is not favorable for the excitation of the SPP mode. At high frequencies, the electric vector leans and the difference of the spectrum becomes small between the two polarizations. The local field intensity at the dielectric sphere and consequently the enhancement of the Raman scattering intensity are determined mainly by the resonance mode frequencies of the sphere and the interference effect. The enhancement is not large as shown in Fig. 5.

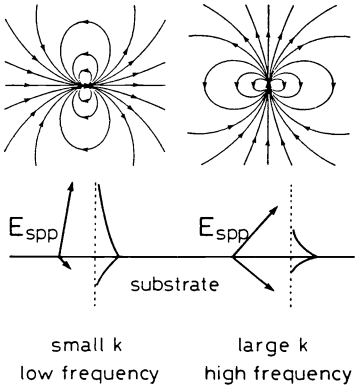

Fig. 4. Schematic diagram of the dipole radiation and the electric vector and the envelope function of the SPP mode.

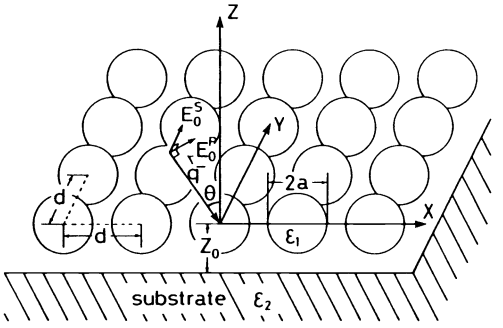

Fig. 6. Geometry of the second model. A square lattice structure is assumed for a two-dimensional array of spheres.

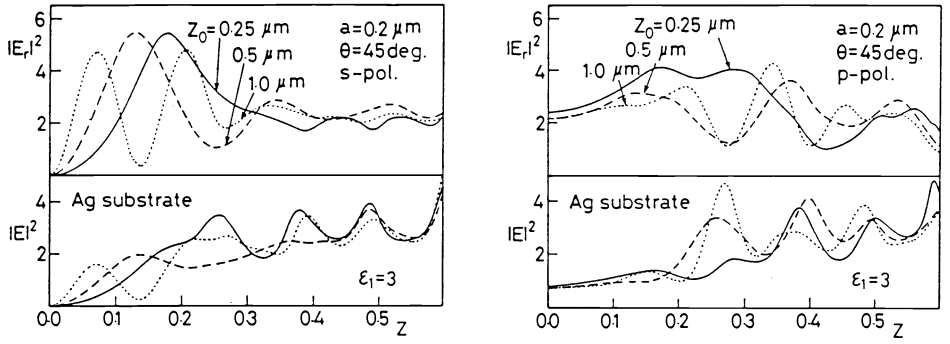

Fig. 5. Local field intensity at the dielectric sphere placed on a metal substrate.

A TWO DIMENSIONAL ARRAY OF DIELECTRIC SPHERES ON A SUBSTRATE

Next, we consider a two-dimensional array of dielectric spheres placed on a flat substrate. The model is shown in Fig. 6. We assumed a square lattice with lattice constant d. Substrate is absent in Figs. 7a and 7b, which summarize the effects of the resonance modes on various electromagnetic quantities; the integrated density of states for the EM field, the specular reflectivity, the electric field intensity averaged inside the sphere, its normal component averaged on the surface, and the enhancement factor of the Raman intensity by the adsorbed molecules observed from the direction of the specular reflection. Solid curves are for p-polarization and the dotted curves are for s-polarization. In this system, the scale of the frequency is changed and is defined by the lattice constant ($Z = d/\lambda$). We put $a/d = 0.4$, $\varepsilon_1 = 3$, and $\theta = 20$ deg., $\phi = 0$ for Fig. 7a and 45 deg. for Fig. 7b. When I.D.S. increases sharply, a resonance mode is excited. The singularity at $Z = 0.74$ in Fig. 7a or $Z = 0.82$ in Fig. 7b comes from the first multi-channel threshold, that

is, below this frequency only specular reflection or transmission occurs, while above this, diffracted waves coexist. The most important fact is, when the resonance modes are excited, the local field intensity is enhanced and its peak value approaches 100. As a result, the Raman intensity is enhanced by almost four orders of magnitude. While the local field intensity is characterized by the symmetry of the resonance mode, the dipole field of the adsorbed molecule has both s- and p-characters. Therefore, the Raman spectrum has singularities at both resonance frequencies.

The resonance-mode frequencies are obtained as the peak frequencies of the local field intensities. By changing the incidence angle, the dispersion relation of the resonance mode is obtained by plotting resonance frequencies versus momentum component parallel to the surface. The result is shown in Fig. 8a. Abscissa is the wavevector component parallel to the surface scaled by the reciprocal lattice vector $K = 2\pi/d$. For comparison, an empty-lattice band structure for a localized mode of a dielectric slab with the same dielectric constant is shown in Fig. 8b. The thickness of the slab is chosen such that the

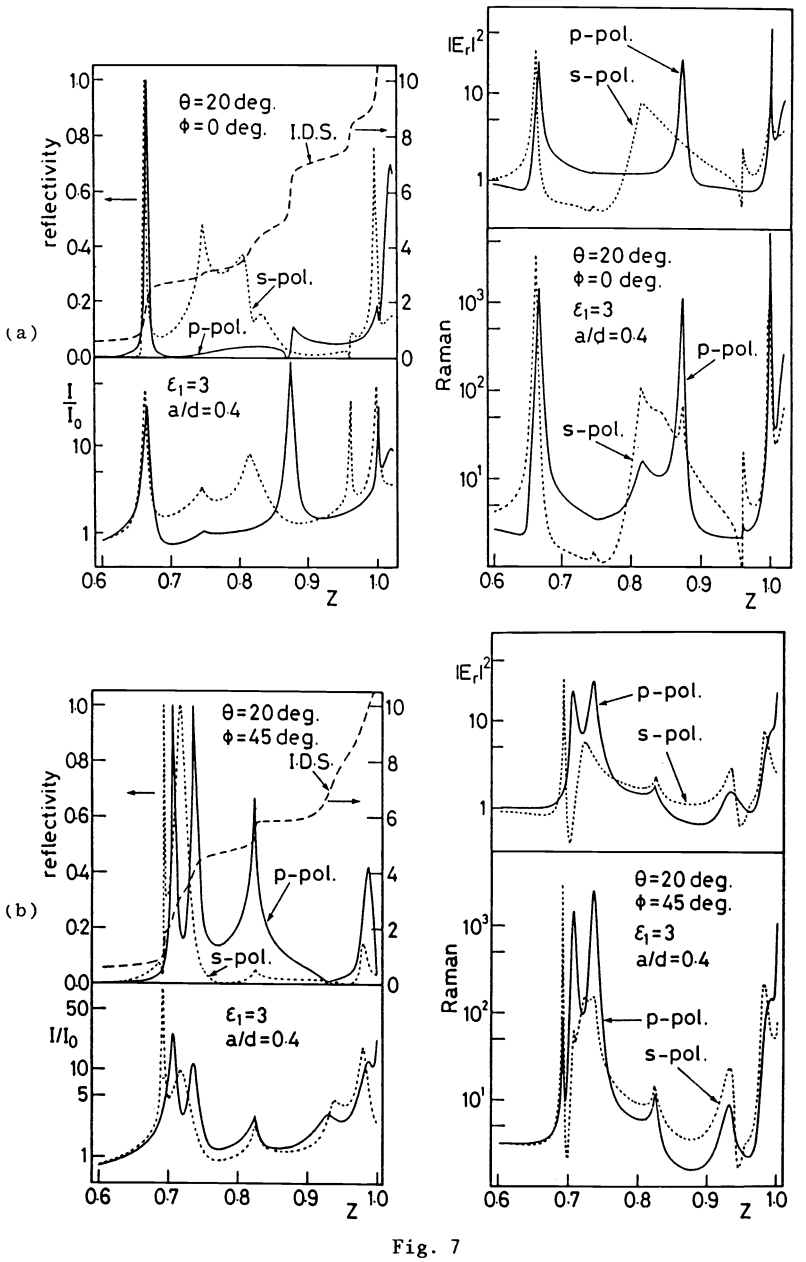

Fig. 7

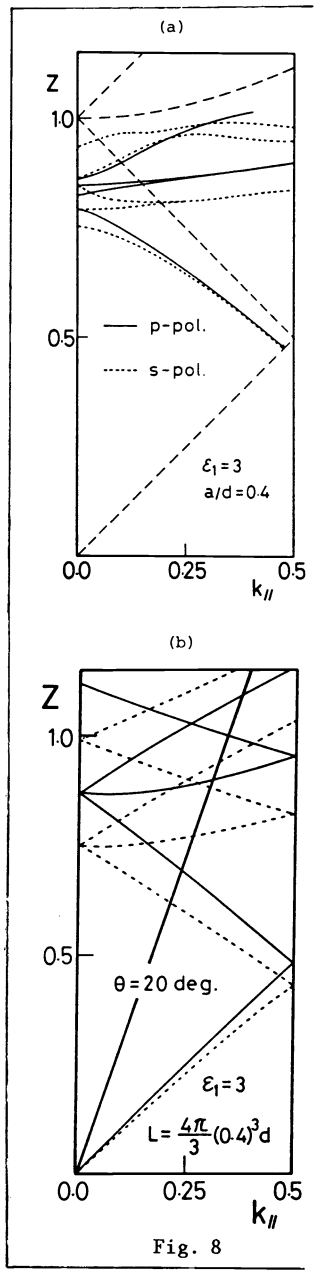

Fig. 8

Fig. 7. Effects of the resonance modes on various electromagnetic quantities. (a): azimuthal angle is zero. (b): azimuthal angle is 45 deg.

Fig. 8. Dispersion relation of the resonance modes. (a): For a two-dimensional array of dielectric spheres; (b): an empty lattice band structure of localized modes of a thin dielectric slab.

volume is equal to that of the arrayed spheres. The correspondence of the two curves is rather good. That is, the resonance modes of an arrayed dielectric spheres are closely related to the localized modes of a thin dielectric slab with an appropriate thickness. This model explains the following features of the resonance modes: (1) With the increase of the radius or the dielectric constant of the sphere, the effective potential in Eq. (3) becomes more attractive and the frequency of the resonance mode decreases. (2) With the incidence angle, the lowest resonance mode shifts to the low frequency side while the high frequency modes form a complicated band structure. This comes from the mixing of nearby excited states. (3) A dispersion curve of an excited state of the localized mode of a slab starts on the line $\omega = ck_{\|}$, i.e., a new resonance mode appears at multi-channel thresholds. Thus, as we have seen, the character of the resonance mode of a single sphere is completely changed by the multiple scatterings between spheres and the resonance modes of an arrayed spheres are closely related to the localized modes of a thin dielectric slab.

Having clarified the character of the resonance mode, we next focus on the substrate effect. In Fig. 9, a dielectric substrate is assumed. The dielectric constant of the sphere is fixed and the distance Z_0 is chosen to be half the lattice constant except for the figure at the bottom where we put $Z_0 = d$. For the figure at the top, substrate is not present. With the increase of the substrate dielectric constant (ε_2), the width of the resonance mode increases and the peak intensity is reduced by an order of magnitude. As the dielectric substrate is equivalent to an attractive potential, the envelope of the resonance mode extends toward the substrate. This effect reduces the local field intensities. When the distance is increased to the lattice constant, the substrate effect becomes negligible, except a sharp peak appearing at Z = 0.94. This peak originates from the excitation of a resonance mode by the diffracted wave which is reflected back to the array by the substrate. This calculation shows that, the resonance mode is confined to a narrow region of thickness less than the lattice constant and the substrate effect is important at short distances.

The effect of a metal substrate is shown in Fig. 10 for $Z_0 = d$. Silver is chosen as the substrate. The average of the local field intensity is shown at the top of the figure. In the middle, we show the energy absorbed inside the substrate and the bottom figure shows the Raman enhancement factor. As the distance Z_0 is large here, the interaction between the resonance mode and the SPP mode is expected to be weak. In fact, the intensity enhancement spectrum is almost the same as that for the case without substrate. The lowest p-mode is nearly degenerate with the s-mode and there are in total three p-modes in the frequency range investigated. The sharp absorption peaks at Z = 0.74 and Z = 1 are

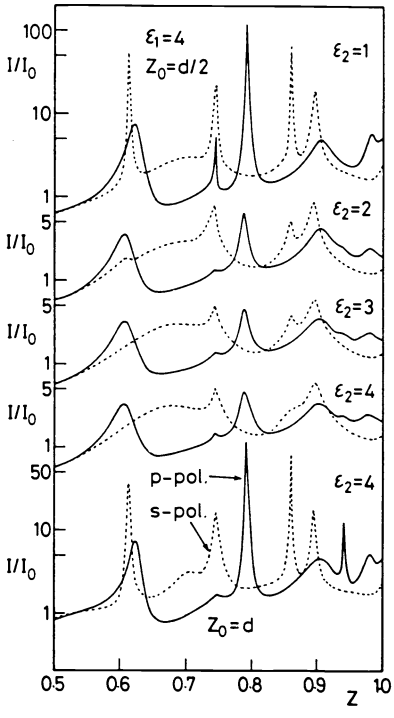

Fig. 9. Averaged local field intensity as a function of the substrate dielectric constant.

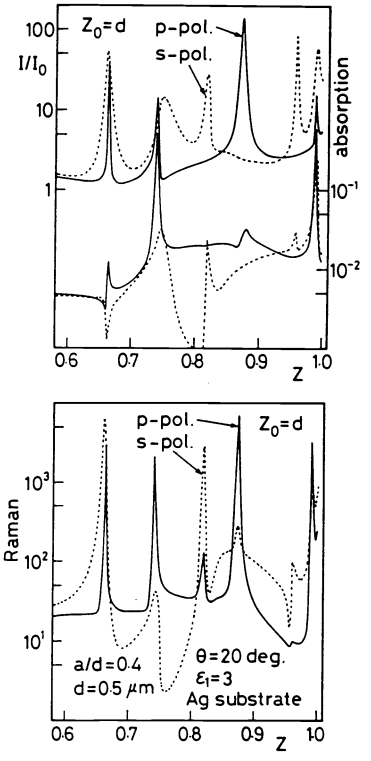

Fig. 10. Effect of the metal substrate for local field intensity and Raman enhancement factor at Z_0=d. Electromagnetic energy dissipated inside the substrate is also shown.

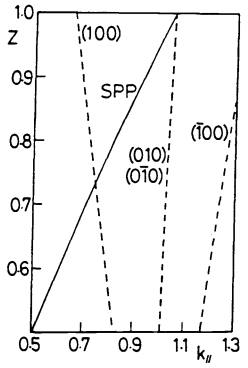

Fig. 11. Dispersion curves of SPP and evanescent waves from the periodic array.

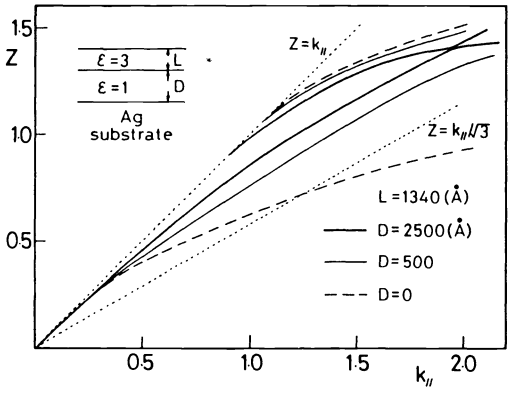

Fig. 13. Dispersion curves of localized modes for a dielectric slab placed on a metal substrate.

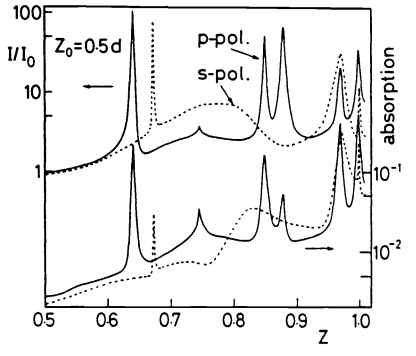

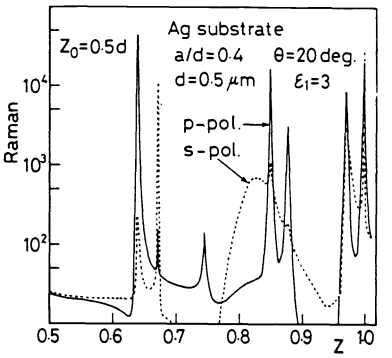

Fig. 12. The same quantities as Fig. 10 at $Z_0 = d/2$.

explained by the resonance excitation of the SPP modes. The solid curve and the dashed curves of Fig. 11 show the dispersion relations of the SPP mode and the evanescent waves of the arrayed spheres. The corresponding reciprocal lattice vectors are inserted. When two curves cross with each other, the energy-momentum conservation is satisfied and the SPP modes are excited by the evanescent waves. The frequencies are equal to those of the absorption peaks in Fig. 10.

On the other hand, when the distance is decreased to half the lattice constant, as shown in Fig. 12, the coupling of the two modes increases and further enhancements are realized for the local field intensity and the Raman scattering efficiency. In the spectrum, there occurs a low frequency shift at Z = 0.64 and splittings around Z = 0.87 and Z = 0.98. As the SPP mode is p-polarized, the coupling is strong for p-polarization. These features of the coupled mode frequencies are again explained by the localized modes of a dielectric slab placed on a metal substrate. We show in Fig. 13 the dispersion relations of p-polarized localized modes. In the calculation, the imaginary part of the dielectric constant is neglected. The bold curves correspond to the present parameters. At low frequencies the two dispersion curves, the dispersion curves of the SPP mode and the localized mode of the slab, are close to each other. Because of their repulsive interaction, one of the mode is pushed up and disappears and the other mode is pushed down. At high frequencies, there exists SPP-like mode. Thus, this model explains the low frequency shift of the low lying modes and their splittings at high frequencies.

The character of the localized mode depends on the distance D and the frequency Z and is best seen by the envelope function of the localized modes. In Figs. 14a and 14b, we show the spatial dependence of the electric-field component parallel to the surface for Z = 0.5 and Z = 1.0. The horizontal bold (dashed) lines show the region of the dielectric slab (metal substrate) and dotted lines indicate the vacuum. The amplitudes are scaled such that $E_{||} = 1.0$ at the metal surface. For Z = 0.5, the amplitude is large in the slab, i.e., the coupled mode has a character of localized mode of the dielectric slab disturbed by the metal substrate. For Z = 1.0, there are two modes for D = 2500 A. The mode with smaller wavevector ($k_{||} = 1.03$) is SPP-like and the other mode ($k_{||} = 1.22$) has large amplitude in the dielectric slab. When the distance is decreased, the latter mode changes its character continuously and becomes SPP-like which exists at the metal-dielectric interface at D = 0.

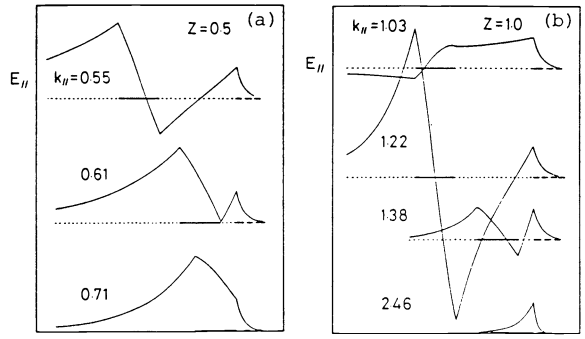

Fig. 14. Envelope of the local mode for a dielectric slab placed on a metal substrate. The electric field component parallel to the surface is shown for p-polarization. (a): Z = 0.5. (b): Z = 1.0.

CONCLUSION

In this paper, various features of the resonance mode are reviewed for a dielectric sphere and an array of dielectric spheres placed on a flat substrate.

When a sphere is placed on a metal substrate, the substrate effect is explained by the following mechanism. The scattered wave from the sphere is expressed by the vector spherical waves with spherical Hankel function. The r-dependence shows that it has evanescent wave components. When the scattered wave reaches the substrate, therefore, it can excite SPP mode which carries the EM energy along the surface out to infinity. As the amplitude of the scattered wave is not so large, the effect of the substrate is small.

For a two-dimensional array of spheres, the feature of the resonance mode is close to that of the localized mode of a dielectric slab and the local field is enhanced by the excitation of the resonance mode. When the array is placed on a dielectric substrate, the substrate effect is important, i.e., at short distances the enhancement of the local field intensity realized by the excitation of the resonance mode decreases by an order of magnitude. This result shows that the local field enhancement at a dielectric surface is not large when microstructures are fabricated by dielectric materials. However, if it is made of a metal, the same mechanism as in the case of SERS becomes effective and the local field is enhanced when SPP-like mode is excited in the metallic microstructures. On the other hand, when the array is placed on the metal substrate, further enhancement is realized for the local field. Thus, Raman scattering is enhanced not only from adsorbed molecules, but also from inside the sphere. This effect is useful for the investigation of lattice vibrations of fine particles. As the character of the resonance mode changes with the frequency, one can choose a mode such that the local field is enhanced inside the sphere or inside the metal substrate. In the former case, nonlinear optical processes are expected inside the dielectric spheres and in the latter case, enhanced second harmonic generation occurs at the metal surface.

We have used a specific model of a two-dimensional array of dielectric spheres places on a metal substrate. However, the characteristic features of the resonance mode are shown to be similar to that of a dielectric slab placed on a substrate. Thus, the obtained features are expected to be quite general and any periodic microstructures fabricated on a metal surface is expected to show similar characteristics. Therefore, we expect that the local field enhancement by the resonance modes of microstructures will find various applications in surface nonlinear optics.

Acknowledgement The author is grateful to Dr. T. Takemori and Dr. K. Ohtaka for their collaboration.

REFERENCES

1. M. Fleischmann, P. J. Hendra and A. J. McQuillan, Chem. Phys. Lett. 24, 163 (1974): D. L. Jeanmaire and R. P. Van Duyne, J. Electroanal. Chem. 84, 1 (1977): M. G. Albrecht and J. A. Creighton, J. Am. Chem. Soc. 99, 5215 (1977).
2. R. K. Chang and B. L. Laube, CRC Critical Rev. in Solid State and Materials Sciences 10, 1 (1984): A. Otto, in Light Scattering in Solids, eds. M. Cardona and G. Guntherodt, Springer, 1984.
3. A. Wokaun, in Solid State Physics 38, eds. H. Ehrenreich, D. Turnbull and F. Seitz, Academic Press, 1984: M. Moskovits, Rev. of Mod. Phys. 57, 783 (1985).
4. M. Born and Z. Wolf, Principles of Optics, 5th ed., Pergamon, New York, 1975.
5. M. Inoue, K. Ohtaka and S. Yanagawa, Phys. Rev. B25, 689 (1982).
6. M. Inoue and K. Ohtaka, Phys. Rev. B26, 3487 (1982): J. Phys. Soc. Jpn 52, 1457 (1983).
7. M. Inoue, submitted to Phys. Rev. B: T. Takemori, M. Inoue and K. Ohtaka, submitted to J. Phys. Soc. Jpn.
8. J. A. Stratton, Electromagnetic Theory, McGraw Hill, New York, 1941.
9. M. Inoue and K. Ohtaka, J. Phys. Soc. Jpn 52, 3853 (1983).
10. K. Ohtaka and M. Inoue, Phys. Rev. B25, 677 (1982).